Metallurgical Characterization of Buttering Deposits

Dinesh Rathod
Associate Professor,
Department of Mechanical Engineering,
FET, MRIU, Faridabad, Haryana
dineshrathod.fet@mriu.edu.in

Abstract: *The dissimilar metallic joints play a critical and indispensable role in the primary heat transport piping system of nuclear reactors. For economic reason primary pressure vessels are made up of SA508 Cl.3 and transport pipelines are made up of SS304LN. Carbon migration is one of the major problems in the welding of these dissimilar joints. For preventing the carbon migration, use of nickel base metals such as Inconel are suggested for buttering and welding. In the present study, focus was given on identification of carbon migration. Considering the carbon percentage in the Low Alloy Steel, Mild steel with same carbon composition was selected for study and the data will be applied to the Low Alloy Steel and SS304LN welding. The buttering layers were made with Inconel 182 and Ni+Fe alloy using SMAW and GTAW process to establish optimum buttering thickness and optimum number of buttering layers as well.*

I. INTRODUCTION

Dissimilar metal welds are used extensively in the power generation, petrochemical and heavy fabrication industries. The resulting weld interface is both microstructurally and geometrically complex. Carbon diffuses from the low alloy steel and forms carbides in the stainless steel while nickel and chromium diffuse into the low alloy steel so that the interface can generate both decarburized and martensitic zones [1].

There are various options available for consumables and literature have shown that ER309L, Inconel 82, Inconel 182 etc are most suitable for welding of ferritic and austenitic stainless steels. The performances of various filler material have also been evaluated [2-3]. Suitable material would also need to be chosen for buttering layer as much of the success depends on proper selection of buttering material.

Many industries involved in construction of pressure vessels and heat exchangers, petrochemical industries are also in need of development of this technology [4]. This technology may be of interest in welding of main steam lines of power plants.

There have been several studies done in the area of welding of stainless steel and mild steel. Most of these identified problems in welding of these steels and main reasons for failure of these joints have been summarized by Tucker and Everle [5] to be the following:

- Cyclic thermal stresses
- Low Oxidation resistance of low alloy ferritic steel.
- Carbon Migration.
- Metallurgical deterioration caused during service

There has been increasing concerns regarding the integrity of dissimilar metal welds since the cracking incident in the V. C. Summer nuclear plant [6]. Dissimilar pipe welding particularly between Austenitic and Ferritic steels have been carried out by many researchers. These studies have been done particularly keeping the applications at power plants into considerations [2, 7-8].

The joint between ferritic steels and austenitic SS have long been recognized as an area of potential problems, because they can generate large thermal

stresses resulting from difference in thermal expansion characteristics—austenitic SS having a coefficient of thermal expansion (CTE) 30% greater than that of ferritic steels). Thermal cycling during power plant operation plays a major role in the premature service failure of these joints. It has been pointed out by Bhaduri et. al. that the difference in the coefficients of thermal expansion between the base metals and the weld metal generates thermal stresses during the numerous start-ups and shutdowns occurring in an operating power plant. These cyclic stresses superimposed on the residual welding stresses, external loads and internal steam pressure may cause the ultimate service failure of these joints[9].

Inconel-182 buttering is the one used by most researchers while welding SS304 LN and SA 508 Cl-3. Since Inconel-182 contain 13~18 % Cr, there is definitely a tendency for carbon migration. This tendency forces one to build around 6.0 ~ 8.0 mm of buttering, thereby increasing the resource and time consumption and with no guarantee of stopping carbon migration. Nickel and Nickel based alloys are suitable material for restricting the carbon migration. Optimum thickness of Inconel 182 alloy buttering has been decided after XRD and EDEX analysis. However the Ni-Fe alloy first layer thickness may not exceed 2.0mm and Subsequent build-up was made using Inconel-182.

II. EXPERIMENTAL PROCEDURE

Materials, Methods and Consumables

The experimentation was carried out on Mild Steel of 0.227% Carbon as base material of 200 x 50 x 6mm size of plate. In first experimentation, the SMAW process was used for buttering of the Inconel 182 electrode of Ö4mm. The electrodes were baked at 200^{O}C for 1.5 ~ 2hr before the operation. The first layer of buttering and subsequent built-ups were carried out by SMAW process only. The experimentation was carried out manually by keeping the welding speed, feed and arc length constant. The process parameters were established by trial runs and the buttering was carried out at 105 amp current with DCEP polarity. Other experimentation was also carried out on the same base material of Mild Steel with same composition. The first layer of buttering was made by GTAW process and subsequent built-up was made by SMAW process. For this experimentation, GTAW process parameters were established by trial runs and gas flow rate of 15 lit/min, welding speed of 0.15 m/min and current of 90 amps with DCEN were used for the buttering of first layer. The first layer was made by Ni-Fe alloy. Subsequent built-up layers were made by SMAW process and the process parameters were kept same as first experimentation.

In first operations, the four buttering layers were made by SMAW, while in the other experimentation, the first layer was made by GTAW using Ni-Fe alloy and subsequent four layers were made by Inconel 182 alloy with SMAW process.

Specimen Fabrication

The samples were prepared by cutting them in required size for Microstructure analysis, micro-hardness analysis, EDEX analysis and XRD analysis. Samples were cut by abrasive cutter, and then they were polished. Etching was done using Nital and Colour etchant (cold saturated solution of sodium thiosulphate 50.0 ml and potassium metabisulfite 1.0 gm) to reveal black and white and the colour metallography. The samples prepared are shown in fig. 1 and the relative information given in Table 1.

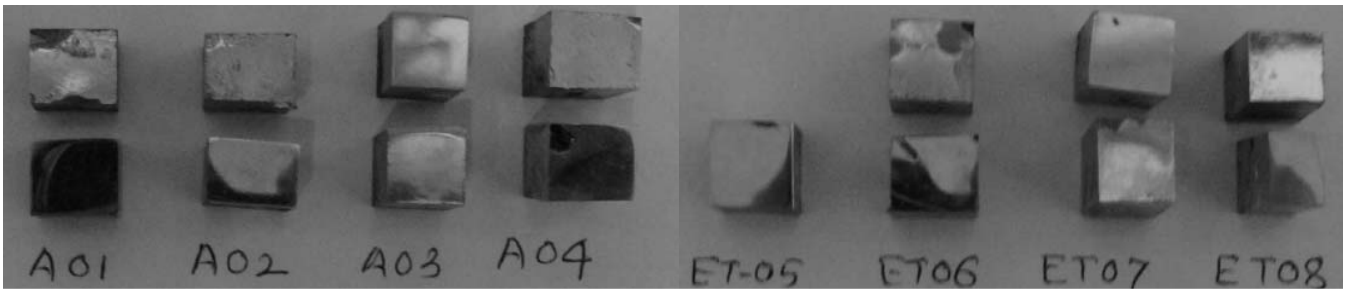

Fig. 1: Specimen showing buttering layers

Table 1: Samples and respective codes showing the number of buttering layers and alloy

	1st layer	2nd layer	3rd layer	4th layer	5th layer
Sample-1(A01)	Inconel-182	-	-	-	-
Sample-2(A02)	Inconel-182	Inconel-182	-	-	-
Sample-3(A03)	Inconel-182	Inconel-182	Inconel-182	-	-
Sample-4(A04)	Inconel-182	Inconel-182	Inconel-182	Inconel-182	-
Sample-5(ET05)	Ni-Fe alloy	Inconel-182	-	-	-
Sample-6(ET06)	Ni-Fe alloy	Inconel-182	Inconel-182	-	-
Sample-7(ET07)	Ni-Fe alloy	Inconel-182	Inconel-182	Inconel-182	-
Sample-8(ET08)	Ni-Fe alloy	Inconel-182	Inconel-182	Inconel-182	Inconel-182

III. RESULTS AND DISCUSSION

Microstructure Analysis

Polished samples were etched with the solution as discussed above. Fig. 2 shows the microstructure of Mild steel material. The blue spot indicates harder phase pearlite while the brownish and yellowish indicates softer phase ferrite. Fig.3 shows the microstructure of Inconel 182 in the first layer with the preferred orientation of the grains. Fig.4 shows the microstructure of fusion interface of mild steel and Inconel 182 in first layer. The fusion boundary is heavily carburised indicated by the black carburised zone at boundary. Fig.5 shows the microstructure of fusion interface of mild steel and Ni-Fe alloy in first layer. The fusion boundary is also carburised but very less as compared to previous case. Very faint black zone of carburised region can be seen near to fusion boundary.

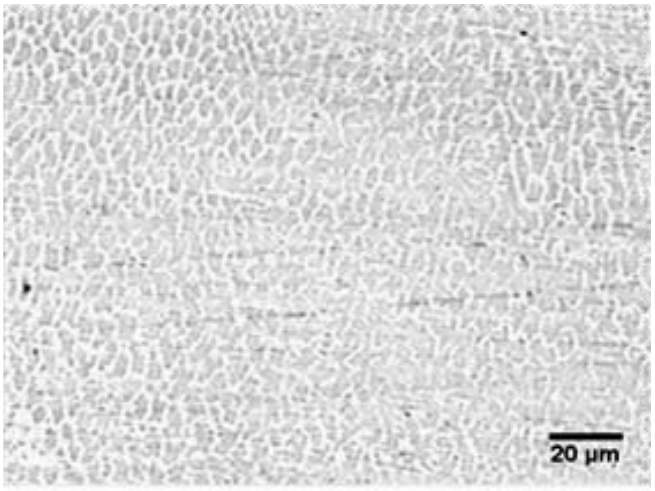

Fig. 3: Inconel 182, Weld Metal in first layer

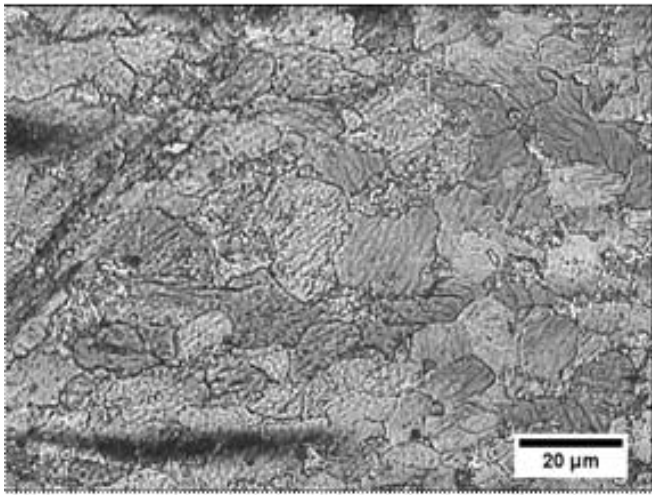

Fig. 2: Mild steel base materials

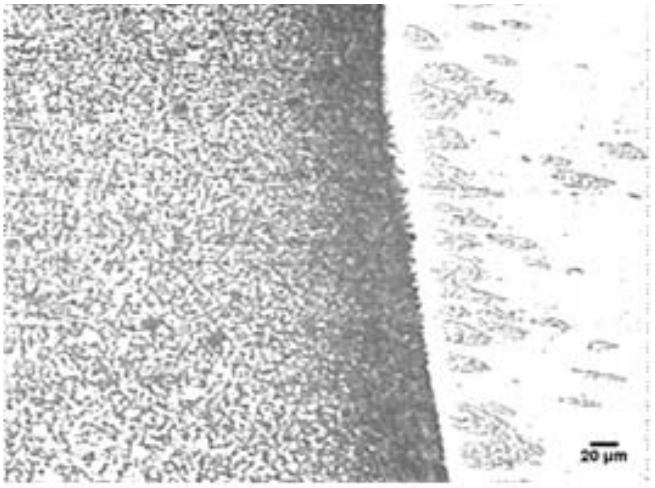

Fig. 4: Fusion interface MS – Inconel 182

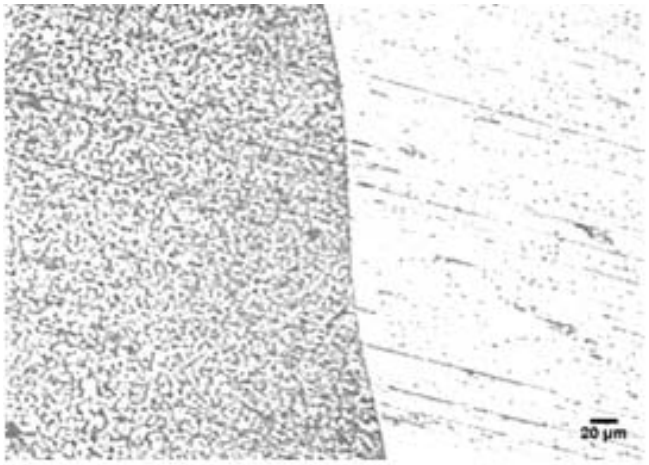

Fig. 5: Fusion Interface MS – Ni-Fe alloy

Fig. 6 shows the microstructure of weld metal of Ni-Fe alloy in the first layer. Microstructure shows how the grains rotate in weld pool. Dendrites also try to rotate, although the grains or dendrites do not actually rotate. As grains are edged out by more favourably oriented grains, they get smaller and eventually can disappear. The grain structure indicates the low heat input and low welding speed [10].

Fig. 6: Ni-Fe alloy, weld metal in first layer

Micro-hardness analysis

Hardness of the material is also indicative of varying carbon content in case of Fe base alloys and metals. More carbon percent will lead to more hardness of the metal. For identification of carbon migration, the first layer and four layer samples were selected for micro-hardness study. Sample A01, A04 from Inconel layers and sample ET05 and ET08 form Ni-Fe and Inconel layers were tested for hardness along with the hardness of base metal and MS HAZ as well. The hardness was measured using 100 gramforce. Table 2 shows the Vicker's Microhardness (HV 100) values of Base metal, HAZ and different buttering layers.

Micro-hardness of HAZ MS found is higher than base metal due to carburization, which was more in case of MS-Inconel layer due to heavy carburization. Hardness was less than Inconel layer but more than base metal in Ni-Fe layer HAZ MS due to very less carburization at the fusion boundary. Hardness found to be highest in case of first layer of Inconel buttering in first layer and it reduces in the fourth layer. In First layer of Ni-Fe alloy, the hardness observed was the lowest one and it slightly increases after the buttering of Inconel 182 in fourth layer, but the hardness of NI-Fe found to be less than the pure Inconel layers.

EDAX Analysis

The purpose was to identify the carbon content in each layer of buttering i.e. to identify the amount of carbon migrated in each layer. The results given by the EDAX machine were full of flaws, as results indicated high carbon wt% in samples. EDAX analysis for elemental identification is reliable only in case of carbon wt% is more than 2%. The results of EDAX analysis were scaled for obtaining a broad idea of the chemical composition by equating the spectro analysis results of

Table 2: Micro-hardness of BM, HAZ and layers

	Average Hardness	Max. Hardness	Min. Hardness	Std. deviation	No. of Indentation
Base Metal	198 HV	215 HV	184 HV	4.56	6
HAZ MS (Inconel layer)	233 HV	272 HV	201 HV	11.83	6
HAZ MS (Ni-Fe layer)	212 HV	220 HV	196 HV	5.72	6
First Layer Inconel (A01)	249 HV	311 HV	195 HV	11.81	9
Four Layer Inconel (A04)	230 HV	248 HV	207 HV	4.8	9
First Layer Ni-Fe (ET05)	204 HV	223 HV	193 HV	5.23	6
Four Layer Ni-Fe + Inconel (ET08)	211 HV	237 HV	174 HV	6.54	8

base metal with EDAX analysis to set a scale. EDAX analysis results are given in Table 3. Fig. 7 indicates the sample of graph obtained during EDAX testing which was later analysed to establish results. All such graphs were analysed according to sample numbers and results are tabulated in Table 3.

Table 3: EDAX analysis results

S No.	Sample	Actual % C	Scaled % C	% Fe	Ni	Cr	Mn	Nb	Ta
1	MS	3.70	0.2270 (Spectro)	99.03	0.035	0.041	0.337	—	—
2	A 01	1.55	0.1089	42.29	33.68	7.96	3.64	1.95	2.38
3	A 02	1.288	0.0899	21.13	49.11	10.81	5.16	2.19	2.13
4	A 03	0.86	0.0604	10.99	58.06	12.72	6.45	1.71	2.45
5	A 04	0.92	0.0646	13.03	56.35	12.37	6.24	1.75	2.4
6	ET 01	0.913	0.0523	36.47	39.09	8.08	3.93	2.11	2.67
7	ET 02	0.919	0.0629	15.75	54.76	10.95	4.86	1.95	2.26
8	ET 03	0.912	0.0611	11.31	59.36	12.37	5.91	1.79	3.1
9	ET 04	0.862	0.0602	8.99	62.05	13.23	6.59	2.12	3

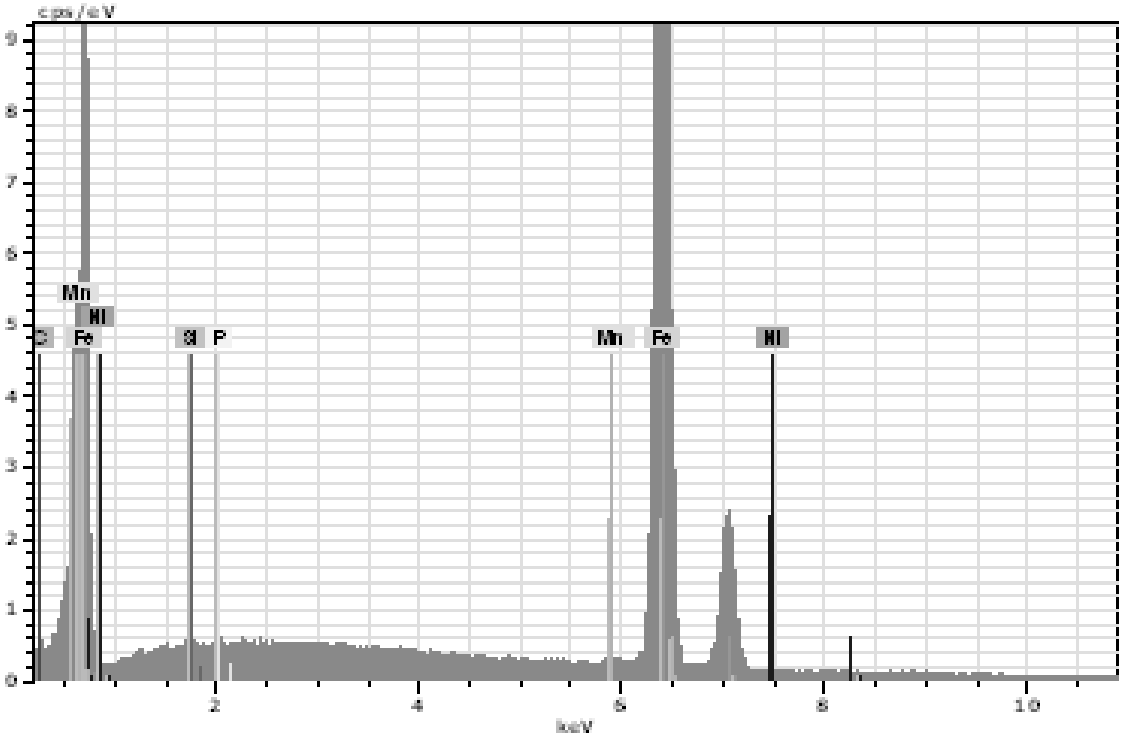

Fig. 7: Graph showing elemental intensity

The carbon wt% found to be 0.1089 in single layer of Inconel 182 while it was reducing when numbers of layers were increased and it was 0.646 in forth buttered layer. In first Inconel layer, weld metal causes the mixing of Inconel with base metal so that wt % of Carbon and iron found to be higher and chromium and Nickel found to be lesser, while in fourth layer wt % of carbon, iron reduced and chromium, Nickel increased.

In Ni-Fe first layer, wt % carbon reduced remarkably to 0.523 and Nickel, iron wt% nearly be equal as low heat input was provided so base metal dilution was less. In subsequent layers carbon wt % increased slightly due to Inconel as carbon pickup by chromium. In fourth buttering layer carbon % found to be 0.0602 while iron, Nickel and chromium % were found to be 8.99, 62.05 and 13.23 respectively.

a) Single layer buttering (sample-1: A01)

XRD Analysis:

The test performed for four samples. First with single layer buttering of Inconel-182 (sample 1-A01), second is four layers of Inconel-182 (sample 4-A04), third is single layer Inconel-182 with initial layer of Ni-Fe alloy (sample 5-ET05) and fourth is four layer Inconel-182 with initial layer of Ni-Fe alloy (sample 8-ET08). The Peak list for various specimens used in the study is presented in the Table 4 – Table 7.

Similarly the XRD profile of the specimens are analysed with the help of peaks observed in the XRD profiles and can be seen from Fig. 8 – Fig. 11.

Table 4: Peak List for specimen A01

Pos.[°2Th.]	Height[cts]	FWHM[°2Th.]	d-spacing[Å]	Rel.Int.[%]
43.6152	3278.20	0.2614	2.07353	73.44
50.7598	4463.83	0.2634	1.79717	100.00
74.7061	626.70	0.3479	1.26960	14.04
90.7223	1673.69	0.3168	1.08256	37.49
96.0818	66.81	0.5890	1.03587	1.50

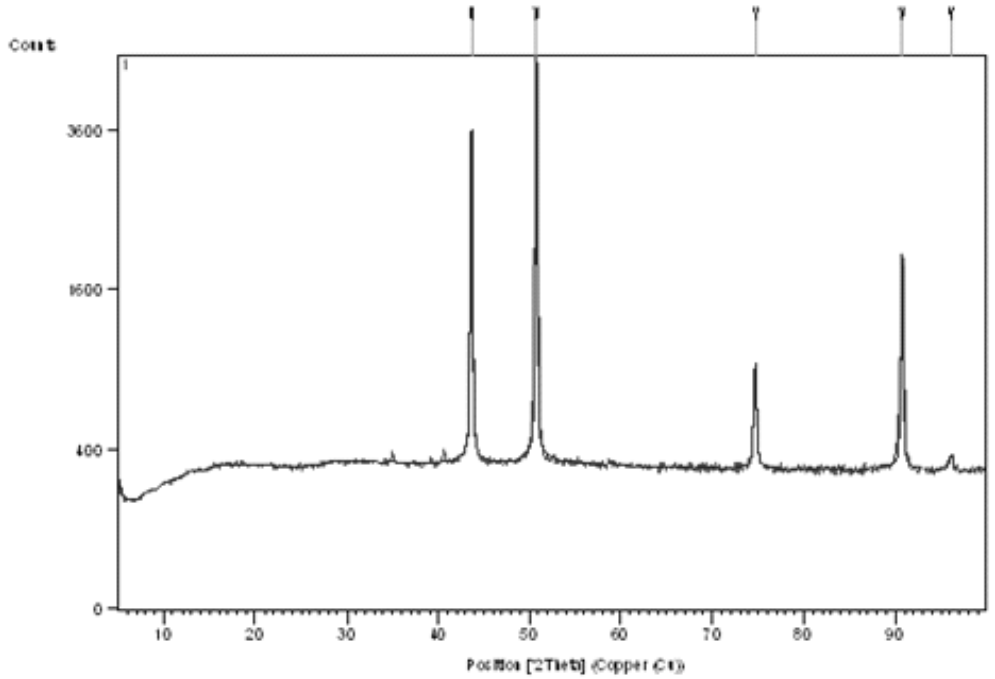

Fig. 8: XRD profiles for specimen A01

Analysis

For peak number two – pos 50.7598 (°2Th)

d-spacing – 1.79719 From Software data – Ref: 09-0122pdf

Matched with d(H) = 1.800 for $Cr_{22}C_6$ chromium carbide with system C

Cell parameter given in software: a=10.63

Calculated value: d spacing = $a/ (h^2+k^2+l^2)^{0.5}$

From software chart: for d(A)= 1.800 , h=5, k=3, l=1

$1.79717 = a/ (5^2+3^2+1^2)^{0.5}$

Calculated a=10.632, it is exactly matched with the given value of a in software chart.

Formed carbide is chromium carbide (Cr rich $Cr_{22}C_6$) of cubic crystal system.

b) Four Layer buttering (sample-4: A04)

Table 5: Peak List of specimen A04

Pos.[°2Th.]	Height[cts]	FWHM [°2Th.]	d-spacing [Å]	Rel. Int. [%]
43.7131	614.75	0.4820	2.06911	1.95
45.6407	78.82	0.3930	1.98611	0.25
50.9276	31498.13	0.3111	1.79164	100.00

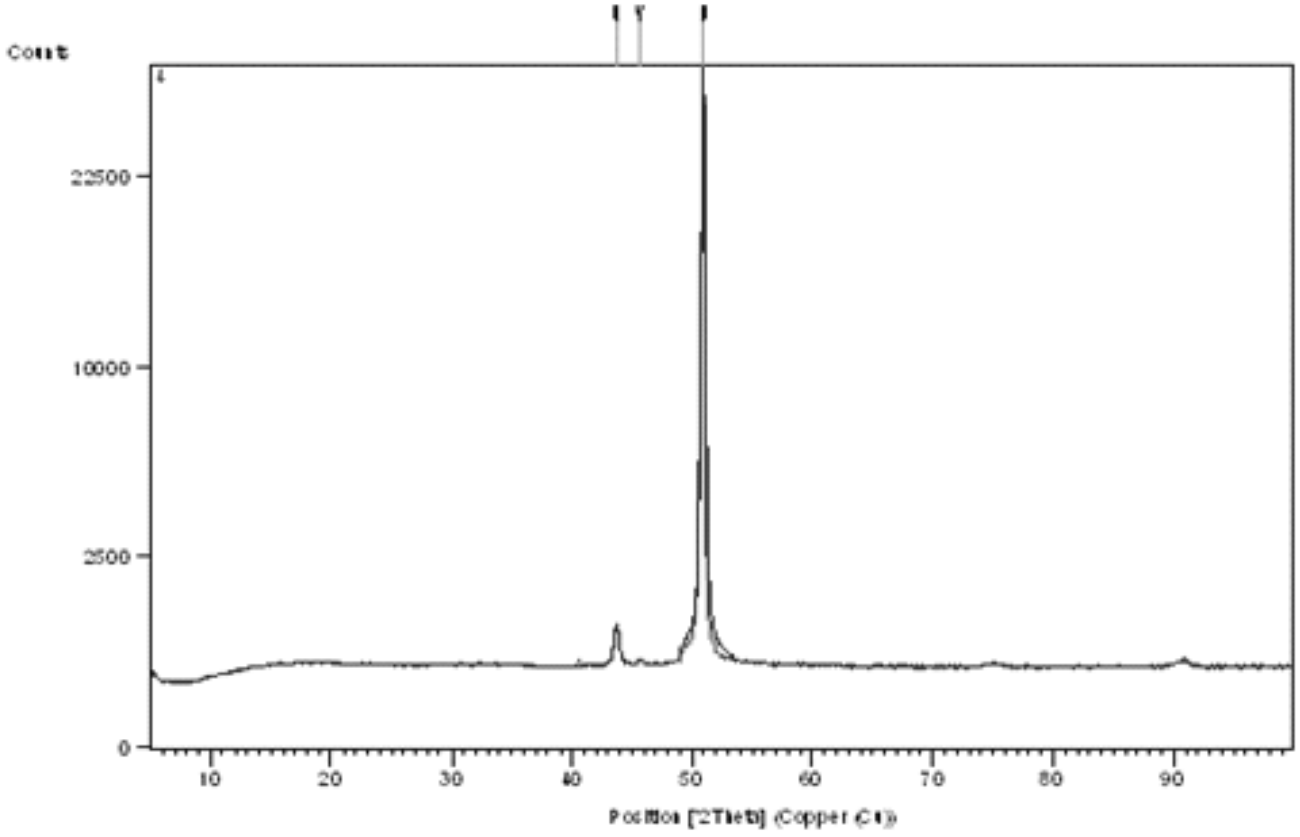

Fig. 9: XRD profiles of specimen A04

Analysis

For peak number three – pos 50.9276 (°2Th)

d-spacing – 1.79164 From Software data – Reference: 09-0122pdf

Matched with d(H) = 1.800 for $Cr_{22}C_6$ chromium carbide with system C

Cell parameter given in software: a=10.63

Calculated value: d spacing = $a/ (h^2+k^2+l^2)^{0.5}$

From software chart: for d(A)= 1.800 , h=5, k=3, l=1

$1.79164 = a/ (5^2+3^2+1^2)^{0.5}$

Calculated a = 10.600, it is matched with the given value of a in software chart.

Formed carbide is chromium carbide (Cr rich $Cr_{22}C_6$)of cubic crystal system.

c) Single layer buttering with Ni-Fe alloy (sample 5-ET05)

Table 6: Peak List of specimen ET05

S. No	Pos.[°2Th.]	Height[cts]	FWHM[°2Th.]	d-spacing[Å]	Rel.Int.[%]
1	20.2721	127.23	1.6105	4.37705	1.37
2	35.2261	179.76	0.4985	2.54571	1.94
3	40.8743	81.88	1.4179	2.20602	0.88
4	43.6040	9287.91	0.2706	2.07404	100.00
5	50.8054	4984.50	0.3358	1.79566	53.67
6	74.7002	4292.15	0.3126	1.26969	46.21
7	90.5963	955.86	0.4048	1.08374	10.29
8	95.8982	228.81	0.5080	1.03737	2.46

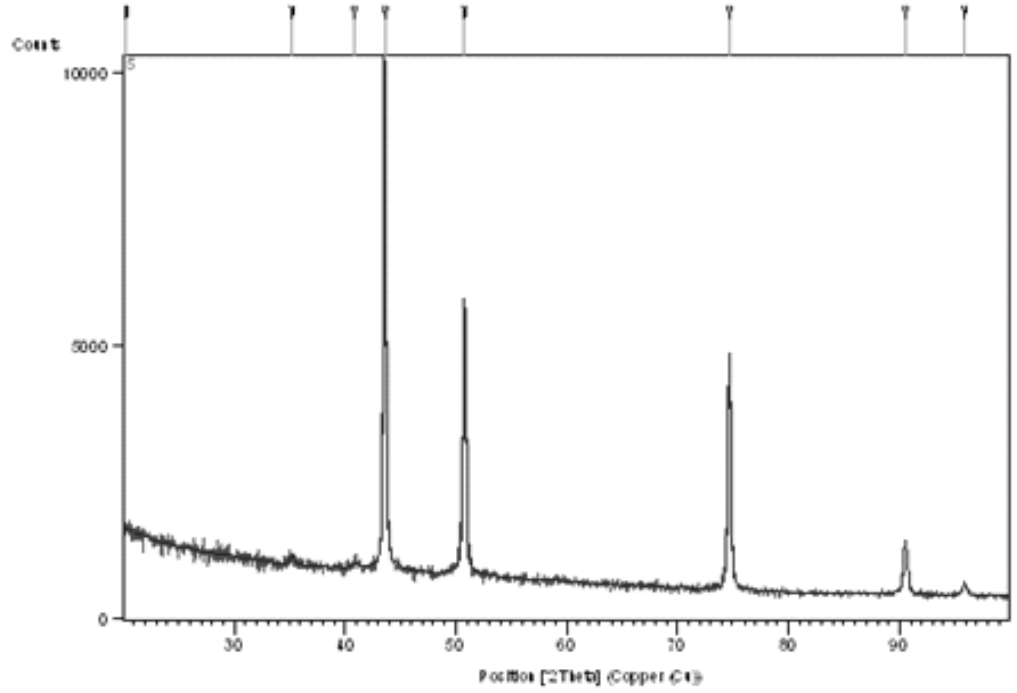

Fig. 10: XRD profiles of specimen ET05

Analysis:

1) For peak at Sl. No. Four – **pos 43.6040** (°2Th)

D-spacing – 2.07404 From Software data – Refer: 31-0619pdf

Matched with d (H) = 2.0800 for Iron Carbide Fe-C (Cubic)

Cell parameter given in software: a=3.60

Calculated value: d spacing = $a/ (h^2+k^2+l^2)^{0.5}$

From software chart: for d (A) = 2.0800, h=1, k=1, l=1

$2.07404 = a/ (1^2+1^2+1^2)^{0.5}$

Calculated a=3.59, it is approximately matching with the given value of a in software chart.

Formed compound is **Iron-carbide (FeC)** of cubic crystal system.

Also from Software data refer: 23-0297pdf for **Fe -Ni (Iron Nickel)**

d spacing= 2.0800, h=1, k=1, l=1

Calculated a= 3.59 and actual a value is 3.596 which is also approximately same.

This is analysed that it may be **Iron carbide (Cubic) or Iron Nickel (Cubic).**

d) Four Layers of buttering with Ni-Fe alloy (Sample-8: ET08)

2) For peak at Sl. No. five position- **pos 50.8054** (°2Th)

d-spacing – 1.79566 From Software data – Refer: 71-0552pdf

Matched with d (H) = 1.8000 for Iron Nickel (Fe-Ni)

Formed compound is **Iron Nickel (Fe-Ni)** of cubic crystal system.

3) For peak at Sl. No. six position- **pos 74.7002** (°2Th)

d-spacing – 1.26969 From Software data – Refer: 23-0297pdf

Matched with d (H) = 1.2700 for Iron Nickel (Fe-Ni): Taenite

Formed compound is **Iron Nickel (Fe-Ni) Taenite** of cubic crystal system.

4) For peak at Sl. No. seven position- **pos 90.5963** (°2Th)

d-spacing – 1.08374 From Software data – Refer: 23-0297pdf

Matched with d (H) = 1.0830 for Iron Nickel (Fe-Ni): Taenite

Formed compound is **Iron Nickel (Fe-Ni) Taenite** of cubic crystal system.

Table 7: Peak List of specimen ET08

Sl.No.	Pos.[°2Th.]	Height[cts]	FWHM[°2Th.]	d-spacing[Å]	Rel.Int.[%]
1	43.7105	6391.96	0.2603	2.06923	8.30
2	50.9161	77054.90	0.2477	1.79202	100.00
3	74.9690	838.35	0.3445	1.26580	1.09
4	90.8298	386.36	0.5961	1.08156	0.50

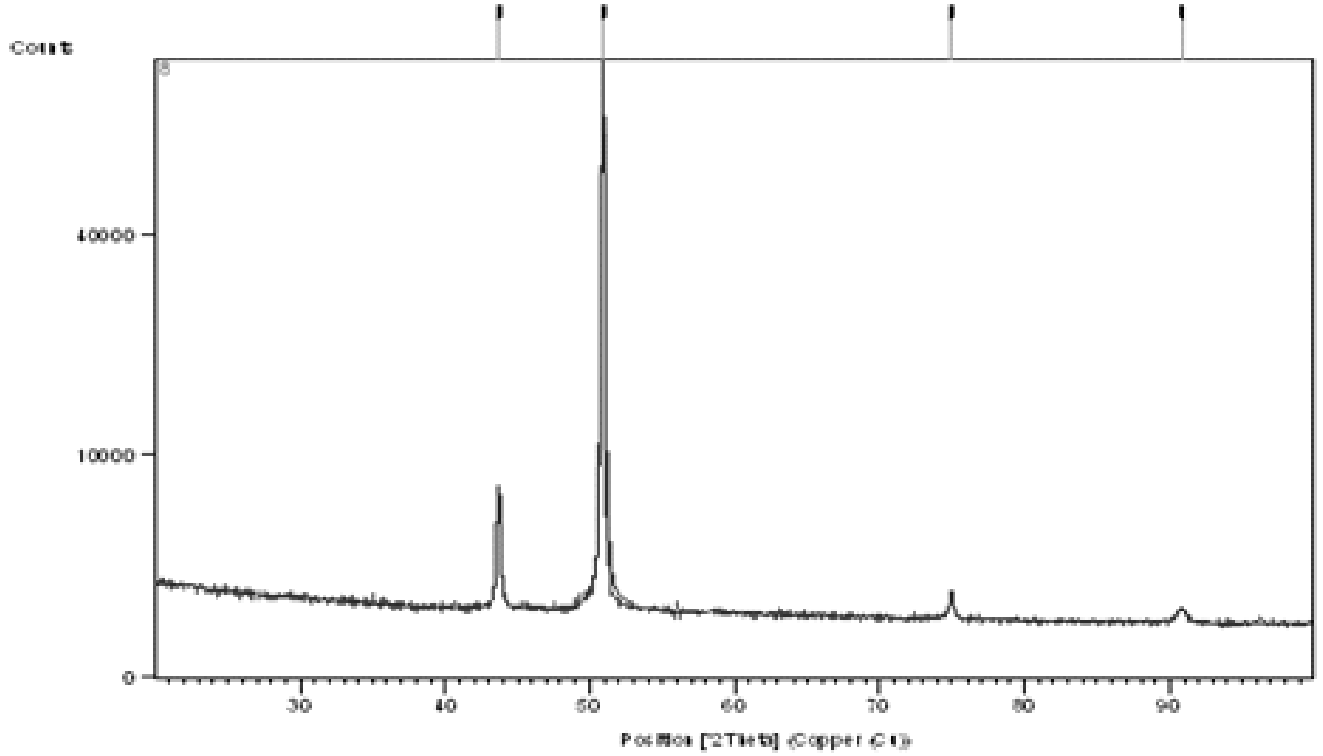

Fig. 11: XRD profiles of specimen ET08

Analysis:

1) For peak at Sl. No. one – **pos 43.7105** (°2Th)

D-spacing – 2.06923 From Software data – Refer: 05-0708pdf

Matched with d (H) = 2.0630 for sigma Fe-Cr (Orthorhombic)

Cell parameter given in software: a=8.799, c=4.544

Calculated value: d spacing = $a/ (h^2+k^2+l^2)^{0.5}$

From software chart: for d (A) = 2.0630, h=3, k=3, l=0

$2.06923 = a/ (3^2+3^2+0^2)^{0.5}$

Calculated a=8.778, it is exactly matched with the given value of a in software chart.

Formed compound is **(ó) sigma Fe-Cr** Orthorhombic crystal system.

2) For peak at Sl. No. two – **pos 50.9161** (°2Th)

D-spacing – 1.79202 From Software data – Refer: 09-0122pdf

Matched with d (H) = 1.8000 for $Cr_{22}C_6$ of Cubic crystal system

Formed Compound is Carbide precipitates of **$Cr_{22}C_6$** with Cubic crystal system.

IV. CONCLUSIONS

1) From microstructure analysis, it can be concluded that the heavy carburised zone appeared in Inconel buttered layer at the HAS of MS as compared to Ni-Fe alloy initial layer. So carbon migration chances are more in Inconel due to presence of chromium in the initial layer.

2) Micro-hardness of HAZ of MS, first layer and fourth layer of Inconel found to be more than in case of Ni-Fe alloy layer, so it can be conclude that carbon pickup in Inconel is higher than the Ni-Fe first layer.

3) Scaled wt% is indicative about the broad idea regarding chemical composition. Carbon wt% found to be higher in Inconel layers than the Ni-Fe initial layer.

4) From XRD analysis, in Inconel single and four layer samples, $Cr_{22}C_6$ chromium rich carbide compound was identified, hence Chromium carbide formation is usually happed in Inconel 182 layers, while in Ni-Fe initial layer, Iron Carbide, Iron Nickel (Teanite) compounds were observed and in subsequent fourth layer of Inconel over Ni-Fe , sigma (Fe-Cr)phase and $Cr_{22}C_6$ precipitate observed. No chromium rich carbide compound observed in Ni-Fe buttered layers.

Acknowledgement

Author would like acknowledge the help and guidance supported by Prof. Sunil Pandey (IIT Delhi) for research work carried out at Welding research Lab of Department of Mechanical Engineering, IIT Delhi.

REFERENCES

[1]. Rowe, M.D., T.W. Nelson, and J.C. Lippold, Hydrogen-induced cracking along the fusion boundary of dissimilar metal welds. Welding Journal, 1999. **78**(2): p. 31S-37S.

[2]. Das, C.R., et al., Selection of filler wire for and effect of auto tempering on the mechanical properties of dissimilar metal joint between 403 and 304L(N) stainless steels. Journal of Materials Processing Technology.

[3]. Sireesha, M., et al., A comparative evaluation of welding consumables for dissimilar welds between 316LN austenitic stainless steel and Alloy 800. Journal of Nuclear Materials, 2000. **279**(1): p. 65-76.

[4]. Missori, S. and C.Koerber, Laser beam welding of austenitic–ferritic transition joints. Welding Journal, 1997. **76**(3): p. 125s-134s.

[5]. Tucker, J.T. and F. Everle, Develepment of a Ferretic-Austenitic Weld joint for Steel Plant Applications. Welding Journal, 1956. **35**(11): p. 529s-540s.

[6]. NRC, Crack in weld area of reactor coolant system hot leg piping at V.C. Summer, in 2000 NRC Information Notice 2000-17.

[7]. Sireesha, M., et al., Microstructural features of dissimilar welds between 316LN austenitic stainless steel and alloy 800. Materials Science and Engineering A, 2000. **292**(1): p. 74-82.

[8]. Nelson, T.W., J.C. Lippold, and M.J. Mills, Nature and Evolution of the Fusion Boundary inFerritic-Austenitic Dissimilar Metal Welds —Part 2: On-Cooling Transformations. Welding Journal, 2000(10).

[9]. Bhaduri, A.K., et al., Transition metal joints for steam generators—An overview. International Journal of Pressure Vessels and Piping, 1994. **58**(3): p. 251-265.

[10]. ASM Handbook Vol. 06 - Welding, Brazing and Soldering.

❐